

Partition Function Zeros of a Restricted Potts Model on Self-Dual Strips of the Square Lattice

Shu-Chiuan Chang^a and Robert Shrock^b

(a) *Department of Physics
National Cheng Kung University
Tainan 70101, Taiwan and*

(b) *C. N. Yang Institute for Theoretical Physics
State University of New York
Stony Brook, N. Y. 11794*

We calculate the partition function $Z(G, Q, v)$ of the Q -state Potts model exactly for self-dual cyclic square-lattice strips of various widths L_y and arbitrarily great lengths L_x , with Q and v restricted to satisfy the relation $Q = v^2$. From these calculations, in the limit $L_x \rightarrow \infty$, we determine the continuous accumulation locus \mathcal{B} of the partition function zeros in the v and Q planes. A number of interesting features of this locus are discussed and a conjecture is given for properties applicable for arbitrarily great width. Relations with the loci \mathcal{B} for general Q and v are analyzed.

PACS numbers: 05.20.-y, 64.60.Cn, 75.10.Hk

I. INTRODUCTION

The Q -state Potts model has served as a valuable model for the study of phase transitions and critical phenomena [1]-[3]. On a lattice or, more generally, on a graph G with n sites (vertices), at temperature T , this model is defined by the partition function

$$Z(G, Q, v) = \sum_{\{\sigma\}} \exp(K \sum_{\langle ij \rangle} \delta_{\sigma_i, \sigma_j}) \quad (1.1)$$

where $\sigma_i = 1, \dots, q$ are the classical spin variables on each vertex $i \in G$, $\langle ij \rangle$ denotes pairs of adjacent vertices, $K = \beta J$ where $\beta = (k_B T)^{-1}$, and J is the spin-spin coupling. We define

$$a = e^K, \quad v = a - 1 \quad (1.2)$$

so that v has the physical range of values $0 \leq v \leq \infty$ and $-1 \leq v \leq 0$ for the ferromagnetic and antiferromagnetic cases $J > 0$ and $J < 0$, respectively. The (reduced) free energy per site is $f = -\beta F = \lim_{n \rightarrow \infty} n^{-1} \ln Z(G, Q, v)$. Aside from the $Q = 2$ Ising special case on two-dimensional lattices, the free energy of the model has never been computed exactly for general Q and v on lattices of dimensionality $d \geq 2$, although the critical behavior is understood for $d = 2$. In view of this lack of exact solutions for $d \geq 2$, there is continuing value in studying the case of lattice strips of finite width L_y and arbitrarily great length L_x , with various boundary conditions. Although these are quasi-one-dimensional systems, and the resultant free energy does not exhibit a phase transition at any finite temperature, they are nevertheless useful for the exact results that can be obtained and the insights that one can gain concerning the properties of the model as a function of Q and v . Among these exact results are the partition function zeros and the loci that they form in the limit $n \rightarrow \infty$. These loci are determined by the equality in magnitude of the eigenvalues of the transfer

matrix with maximal modulus and hence are also called the set of equimodular curves. (Here “curves” is used in a generic sense; these loci can also include line segments.) In previous works we have presented exact calculations of the Potts model partition function for arbitrary Q and v on such strips and have also investigated various special cases [4]. One type of special case is provided by considering requiring Q and v to satisfy some functional relation.

In this paper we consider the Potts model on self-dual cyclic square-lattice strips of various widths L_y and arbitrarily great lengths L_x , with the variables Q and v restricted to satisfy, in terms of the variable $\zeta_{sq} = v/\sqrt{Q}$, the relation

$$\zeta_{sq} = 1. \quad (1.3)$$

It will actually be convenient to consider the square of this condition, namely,

$$Q = v^2. \quad (1.4)$$

The condition (1.3) is the condition for the phase transition temperature of the Potts ferromagnet on a two-dimensional square lattice, i.e., $k_B T_c = J/\ln(1 + \sqrt{Q})$. (The transition is second-order for $0 < Q \leq 4$ and first-order for $Q > 4$.) For the $L_x \rightarrow \infty$ limits of these strips we exactly determine the continuous accumulation loci \mathcal{B} of the partition function zeros in the v and Q planes.

Because of the quasi-one-dimensional nature of the infinite-length strips that we consider, the significance of the condition (1.3) or (1.4) is not that the Potts ferromagnet has a phase transition at this temperature, but rather that it is a self-dual point; the partition function satisfies the duality relation

$$Z(G, Q, v) \propto Z(G^*, Q, v_d), \quad (1.5)$$

where G^* denotes the planar dual to G and

$$v_d = \frac{Q}{v}, \quad \text{i.e.,} \quad \zeta_d = \frac{1}{\zeta}. \quad (1.6)$$

If $G = G^*$, as is the case with our self-dual square-lattice strips, and if $v = v_d$, then, up to a multiplicative factor which will not be important here, the partition function is transformed to itself under duality. The properties of the Potts model for the submanifold of values of Q and v that satisfy the condition (1.4) are thus of general interest even if the model does not exhibit a phase transition at the corresponding temperature.

II. PRELIMINARIES

In this section we review some background which will be used in the subsequent portion of the text. A graph $G = G(V, E)$ is defined by its vertex set V and its edge set E (where V should not be confused with the temperature-like Boltzmann variable v). The number n of vertices of G is denoted as $n = n(G) = |V|$ and the number of bonds (edges) of G as $e(G) = |E|$. The degree of a vertex is defined as the number of edges that connect to it. The Potts model can be generalized from non-negative integer Q to non-negative real Q via the relation [5]

$$Z(G, Q, v) = \sum_{G' \subseteq G} Q^{k(G')} v^{e(G')} \quad (2.1)$$

where G' is a spanning subgraph of G , i.e., $G' = (V, E')$ with $E' \subseteq E$, and $k(G')$ denotes the number of connected components of G' . This relation also allows one to consider v and Q to be complex, as will be necessary in analyzing the zeros of $Z(G, Q, v)$. A transfer matrix formalism for the Potts model that can be used for real Q was presented in Ref. [6].

Given that one restricts Q and v to satisfy eq. (1.4), one can express $Z(G, Q, v)$ as a function of one variable. Expressing Q as a function of v via eq. (1.4), one obtains $Z(G, v^2, v)$. This has the general form, from eq. (2.1),

$$Z(G, v^2, v) = \sum_{G' \subseteq G} v^{2k(G') + e(G')} \quad (2.2)$$

The alternate procedure, expressing v as a function of Q , is not as convenient, since the formal solution for v involves a sign ambiguity, $v = \pm\sqrt{Q}$. Clearly, since $Z(G, v^2, v)$ is a polynomial in v with real coefficients [7], the set of its zeros and the resultant locus \mathcal{B} are invariant under complex conjugation.

The Potts model partition function is equivalent to an important function in mathematical graph theory, the Tutte polynomial $T(G, x, y)$ [8, 9]:

$$Z(G, Q, v) = (x-1)^{k(G)} (y-1)^{n(G)} T(G, x, y) \quad (2.3)$$

where

$$x = 1 + \frac{Q}{v}, \quad y = 1 + v. \quad (2.4)$$

(We follow standard mathematical notation here; the reader should not confuse these Tutte variables x and y with the longitudinal and transverse strip graph coordinates x and y , since the meaning will be clear from context.) For a planar graph G , the Tutte polynomial satisfies $T(G, x, y) = T(G^*, y, x)$. In terms of Tutte variable, eq. (1.4) reads $(x-1)(y-1) = (y-1)^2$. Since the case $y = 1$, i.e., $K = 0$, is trivial, one may concentrate on the case $y \neq 1$ and divide by $(y-1)$, obtaining the corresponding condition $x = y$. For a self-dual planar graph G such as the lattice graphs that we consider here, $T(G, x, y) = T(G, y, x)$.

The Potts model on a $L_x \times L_y$ section of a lattice is related to quantum algebras, in particular, to the algebra defined by a set of operators U_i satisfying the relations [10]

$$U_i^2 = Q^{1/2} U_i \quad (2.5)$$

$$[U_i, U_j] = 0 \quad \text{if } |i-j| \neq 1 \quad (2.6)$$

$$U_i U_{i\pm 1} U_i = U_i \quad (2.7)$$

where the range of the index i on U_i can be taken to be $1 \leq i \leq 2L_y - 1$. One commonly writes

$$\sqrt{Q} = q + q^{-1} \quad (2.8)$$

where

$$q = e^{i\theta/2} \quad (2.9)$$

so that

$$Q = 4 \cos^2(\theta/2). \quad (2.10)$$

The case where q is a root of unity, i.e., θ/π is rational, will be relevant to our discussion below. We define the root of unity $q_r = e^{i\pi/r}$ and correspondingly

$$Q_r = 4 \cos^2(\pi/r). \quad (2.11)$$

The values Q_r corresponding to the roots of unity q_r are often called Tutte-Beraha numbers; early interest in these arose in studies of the chromatic polynomial $P(G, Q) = Z(G, Q, -1)$, equal to the Potts antiferromagnet at zero temperature [8, 9, 11] (see also [12]). They also play a special role for the finite-temperature Potts model (with either sign of J), as is clear from the fact that the representations of the algebra of eqs. (2.5)-(2.7) are reducible at $Q = Q_r$ [13, 14]. We also define

$$v_r = -2 \cos(\pi/r) \quad (2.12)$$

so that $Q_r = v_r^2$. For $Q = Q_r$ and $v = v_r$, the associated values of the Tutte variables are given by eq. (2.4) as $x_r = y_r = 1 - 2 \cos(\pi/r)$. Calculations of zeros of $Z(G, v^2, v)$ on finite sections of the square lattice found that a subset of these zeros occurred at or near certain Q_r values [19], and, as will be discussed below, we find that the accumulation loci \mathcal{B}_Q cross the real Q axis at certain Q_r values.

III. GENERAL FORM OF $Z(G, Q, v)$ FOR SELF-DUAL CYCLIC SQUARE-LATTICE STRIPS

We focus on strip graphs of the square lattice of length L_x vertices and width L_y vertices with periodic longitudinal boundary conditions and with one additional external vertex connected to each of the vertices on one side of the strip, say the top side. For these graphs the number of vertices is $n = L_x L_y + 1$, which is equal to the number of faces, and the number of edges is $e = 2n$ [15]. The average vertex degree, defined as $2e(G)/n(G)$, is equal to 4, the same value for the square lattice. As regards individual vertices, the external vertex has degree L_x , the L_x vertices on the bottom side of the strip have degree 3, and the $L_x(L_y - 1)$ other vertices have degree 4. These graphs are self-dual, and accordingly we label the boundary conditions as self-dual cyclic boundary conditions (CDBC) and the graphs as $G_{CDBC}[L_y \times L_x]$. The fact that these square-lattice strip graphs maintain the property of self-duality that holds for the (infinite) square lattice makes them particularly valuable to use in this type of study. Furthermore, the periodic longitudinal boundary conditions minimize boundary effects in this direction. To explain one of the most important consequences of these self-dual boundary conditions, we recall that the locus \mathcal{B}_ζ for the Potts ferromagnet on infinite-length, finite-width strips usually extends to $\zeta = \infty$, i.e., $K = \infty$, reflecting the fact that the model has a critical point at $T = 0$ (and zero magnetization for $T > 0$ but nonzero magnetization at $T = 0$). This was, indeed, the case for strips of many different lattices for which we obtained exact determinations of the locus \mathcal{B}_ζ or the equivalent loci \mathcal{B}_v or \mathcal{B}_a (e.g., [24]-[29]). However, as our exact determinations of \mathcal{B}_ζ for infinite-length, finite-width strips of the square lattice with cyclic or free self-dual boundary conditions in Ref. [21] showed, the locus \mathcal{B}_ζ does not extend to $\zeta = \infty$ and is compact in the ζ plane. This difference arises because, owing to the self-duality, it follows that

$$\mathcal{B}_\zeta \text{ is invariant under } \zeta \rightarrow \frac{1}{\zeta}. \quad (3.1)$$

Consequently, for the self-dual strips, \mathcal{B}_ζ passes through the zero-temperature point $\zeta = \infty$ if and only if it passes through the infinite-temperature point, $\zeta = 0$. But it cannot pass through the latter point because the free energy is analytic in the neighborhood of $K = 0$. Thus, for general Q and v , the infinite-length, finite-width self-dual strips share with the (infinite) square lattice both the property of self-duality and the property that \mathcal{B}_ζ is compact in the ζ plane. As we shall show, however, when we restrict Q and v to obey the relation (1.4), the resultant singular locus \mathcal{B}_v , and hence also \mathcal{B}_Q , are noncompact in their respective v and Q planes. We note that finite sections of the square lattice with these CDBC boundary conditions have previously been used for studies of complex-temperature zeros of the Potts model partition function in Refs. [16, 17, 19].

The Potts model partition function has the general

form [20, 21]

$$Z(G_{CDBC}[L_y \times L_x], Q, v) = Q v^{L_x L_y} \sum_{d=1}^{L_y+1} \sum_{j=1}^{n_Z(L_y, d)} \bar{\kappa}^{(d)} (\bar{\lambda}_{L_y, d, j})^{L_x} \quad (3.2)$$

where

$$\kappa^{(d)} \equiv Q \bar{\kappa}^{(d)} = \sum_{j=0}^{d-1} (-1)^j \binom{2d-1-j}{j} Q^{d-j} \quad (3.3)$$

and

$$n_Z(L_y, d) = \frac{2d}{L_y + d + 1} \binom{2L_y + 1}{L_y - d + 1} \quad (3.4)$$

for $d = 1, \dots, L_y + 1$ (and zero for other values of d). The $\bar{\lambda}_{L_y, d, j}$ are eigenvalues of a transfer matrix of the type discussed in Ref. [6]. In terms of the notation of Ref. [21],

$$\bar{\lambda}_{L_y, d, j} \equiv v^{-L_y} \lambda_{L_y, d, j}. \quad (3.5)$$

Since $n_Z(L_y, L_y + 1) = 1$, i.e., there is only one eigenvalue for $d = L_y + 1$, we label it simply as $\bar{\lambda}_{L_y, L_y+1, 1} \equiv \bar{\lambda}_{L_y, L_y+1}$. This eigenvalue is [20, 21]

$$\bar{\lambda}_{L_y, L_y+1} = 1. \quad (3.6)$$

From the general form (3.2) it follows that $Z(G_{CDBC}[L_y \times L_x], v^2, v)$ has a zero of multiplicity at least $L_x L_y + 2 = n + 1$ at $v = 0$. We find that this is an isolated zero for these types of graphs.

The coefficients $\kappa^{(d)}$ can be written as [20, 23]

$$\kappa^{(d)} = \prod_{k=1}^d (Q - s_{d,k}) \quad (3.7)$$

where

$$s_{d,k} = 4 \cos^2 \left(\frac{\pi k}{2d} \right). \quad (3.8)$$

The first few coefficients $\bar{\kappa}^{(d)}$ are $\bar{\kappa}^{(1)} = 1$, $\bar{\kappa}^{(2)} = Q - 2$, and $\bar{\kappa}^{(3)} = (Q - 1)(Q - 3)$. From eq. (3.3) or (3.7) it follows that if $d \geq 3$ and $d = 0 \pmod{3}$, $\bar{\kappa}^{(d)}$ contains the factor $(Q - 1)(Q - 3)$. i.e.,

$$\bar{\kappa}^{(d)} = (Q - 1)(Q - 3) \mu(Q) \quad \text{if } d \geq 3, \quad d = 0 \pmod{3} \quad (3.9)$$

where $\mu(Q)$ is a polynomial of degree $d - 3$. This property will be used later. We also note that if d is even, then $\bar{\kappa}^{(d)}$ contains the factor $(Q - 2)$. The total number of eigenvalues is

$$\sum_{d=1}^{L_y+1} n_Z(L_y, d) = \binom{2L_y + 1}{L_y + 1}. \quad (3.10)$$

For given values of Q , v and d , the eigenvalue with maximum modulus, i.e., the maximal or dominant eigenvalue, is labelled $\lambda_{L_y, d, max}$.

As discussed in (section 2.2 of) Ref. [24], the formal definition for the reduced free energy, f is not adequate for (real, non-negative) non-integer Q because at certain special points Q_{sp} one has the noncommutativity of limits

$$\lim_{n \rightarrow \infty} \lim_{Q \rightarrow Q_{sp}} Z(G, Q, v)^{1/n} \neq \lim_{Q \rightarrow Q_{sp}} \lim_{n \rightarrow \infty} Z(G, Q, v)^{1/n}. \quad (3.11)$$

The definitions of f with these two different order of limits are denoted, as in Ref. [24], f_{nQ} and f_{Qn} . Clearly, no such issue of noncommutativity arises if one restricts to positive integer Q values and uses the original Potts model definition (1.1). However, since we will consider the more general case of positive real Q as encompassed in the formula (2.1), we will have to take account of this noncommutativity.

IV. PARTITION FUNCTION ZEROS AND LOCI \mathcal{B}

A. General

We now determine the loci \mathcal{B} in the v and Q planes, denoted \mathcal{B}_v and \mathcal{B}_Q , for the infinite-length limits of these strip graphs for several widths L_y . We also compare these to zeros calculated for long finite strips. Our procedure is to calculate $Z(G_{CDBC}[L_y \times L_x], v^2, v)$, solve for the locus \mathcal{B}_v as the locus of solutions of degeneracy in magnitude of dominant $\bar{\lambda}_{L_y, d, j}$'s, and then obtain \mathcal{B}_Q via the mapping (1.4). We find that these loci exhibit a number of interesting systematic properties. To explain these, we first discuss our exact solutions for strips of specific widths.

B. $L_y = 1$

In this case, the graph is equivalent to the wheel graph in mathematical graph theory. Using our exact solution for the Potts model partition function on this graph [20, 21, 22], we find that, with $L_x = m$,

$$\begin{aligned} Z(G_{CDBC}[1 \times m], v^2, v) &= \\ &= v^{m+2} \left[\{(\bar{\lambda}_{1,1,1})^m + (\bar{\lambda}_{1,1,2})^m\} + \bar{\kappa}^{(2)} \right] \end{aligned} \quad (4.1)$$

where

$$\bar{\lambda}_{1,1,j} = \frac{1}{2} \left[3 + 2v \pm \sqrt{5 + 4v} \right] \quad (4.2)$$

with $j = 1, 2$ corresponding to \pm , and we have used $\bar{\lambda}_{1,2} = 1$ from eq. (3.6). Here and below the coefficient functions $\bar{\kappa}^{(d)} = \bar{\kappa}^{(d)}(Q)$ are understood to be evaluated on the manifold (1.4).

In the limit $L_x \rightarrow \infty$, we have calculated the exact locus \mathcal{B}_v in the v plane and its image under the mapping (1.4), \mathcal{B}_Q in the Q plane. We find that \mathcal{B}_v consists of the union of (i) a pinched oval that crosses the real v axis at $v = v_3 = -1$ and $v = -2$ with (ii) a semi-infinite line segment on the negative real v axis extending leftward from $v = -2$ to $v = -\infty$. In the region outside of the pinched oval, $\bar{\lambda}_{1,1,1}$ is the dominant eigenvalue. Along the semi-infinite line segment, $\bar{\lambda}_{1,1,1} = \bar{\lambda}_{1,1,2}^*$, so that $|\bar{\lambda}_{1,1,1}| = |\bar{\lambda}_{1,1,2}|$. In the region within the oval, $\bar{\lambda}_{1,2} = 1$ is the dominant eigenvalue. The fact that \mathcal{B}_v does not intersect the positive real axis at any finite point is a general result reflecting the quasi-one-dimensional nature of these infinite-length strip graphs and the consequent property that the free energy is analytic for all finite temperatures. As one moves leftward along the real v axis, the first nonanalyticity that one encounters, at $v = -1$ is precisely the zero-temperature limit of the Potts anti-ferromagnet (with $Q = v^2 = 1$).

The locus \mathcal{B}_Q , shown in Fig. 1, is the union of (i) a pinched oval that crosses the real Q axis at $Q = Q_3 = 1$ and $Q = Q_1 = 4$ (where Q_r was defined in eq. (2.11)) with (ii) a semi-infinite line segment on the real Q axis extending from $Q = 4$ to $Q = \infty$. Note that in terms of the Tutte variables,

$$v = -2, Q = 4 \iff x = y = -1. \quad (4.3)$$

In Fig. 1 we also show partition function zeros calculated for a long finite strip, with $L_x = 40$. (For this length some of the zeros on the positive real have magnitudes too large to be included in the figure.) At $v = -2$ and its image point $Q = 4$, the magnitudes of all three eigenvalues are degenerate and equal to 1. In addition to the isolated zero at $Q = Q_2 = 0$ as discussed above, the partition function has a zero very close to $Q = Q_4 = 2$. This can be understood as a consequence of the fact that in this region $\bar{\lambda}_{1,2,max}$ is dominant, but its coefficient $\bar{\kappa}^{(2)} = Q - 2$ vanishes at $Q = 2$. In Fig. 1 one can also see several real zeros in the interval $Q > 4$; as $L_x \rightarrow \infty$, these and other real zeros in this interval merge to form the semi-infinite line segment on \mathcal{B}_Q .

This calculation provides a simple example of the non-commutativity (3.11). Consider the point $v_{sp} = -\sqrt{2}$, whence $Q_{sp} \equiv v_{sp}^2 = 2$. Now if we first set $Q = 2$ and then take $n \rightarrow \infty$ to calculate f_{nQ} , then, since the coefficient $\bar{\kappa}^{(2)}$ vanishes at this point, the dominant term $\bar{\lambda}_{1,2}^m = 1$ in eq. (4.1) is annihilated. Furthermore, at this point

$$\bar{\lambda}_{1,1,j} = (\sqrt{2} - 1)e^{\pm i\theta} \quad (4.4)$$

where

$$\theta = \arctan\left(\frac{\sqrt{4\sqrt{2} - 5}}{3 - 2\sqrt{2}}\right) \quad (4.5)$$

so that

$$Z(G_{CDBC}[1 \times m], 2, -\sqrt{2}) = 2(-2)^{\frac{m+2}{2}} (\sqrt{2} - 1)^m \cos(m\theta) \quad (4.6)$$

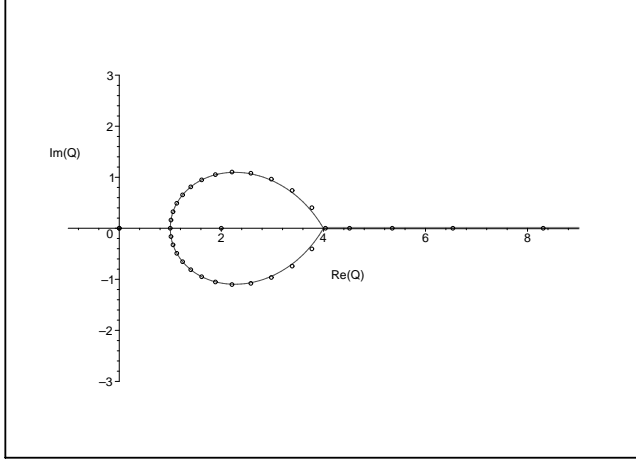


FIG. 1: Locus \mathcal{B}_Q for the Potts model on a $1 \times \infty$ graph with CDBC and $Q = v^2$. This locus includes a semi-infinite line segment on the interval $4 \leq Q \leq \infty$. Partition function zeros are shown for a graph of length $L_x = 40$.

and hence

$$\lim_{n \rightarrow \infty} \lim_{(Q,v) \rightarrow (2, -\sqrt{2})} |Z^{1/n}| = 2 - \sqrt{2} \quad (4.7)$$

With the opposite order of operations, one obtains the different result

$$\lim_{(Q,v) \rightarrow (2, -\sqrt{2})} \lim_{n \rightarrow \infty} |Z^{1/n}| = \sqrt{2} \quad (4.8)$$

where, since there is no canonical phase to pick for the $1/n$ 'th root [24], we just display the modulus.

C. $L_y = 2$

For the width $L_y = 2$ strips with CDBC we use our previous exact calculation of the partition function in Refs. [20, 21] and specialize to the submanifold of variables given by (1.4). From eq. (3.4) there are five $\bar{\lambda}_{2,1,j}$'s, and four $\bar{\lambda}_{2,2,j}$'s, so that, together with the single $\lambda_{2,3}$, the total number of $\bar{\lambda}_{2,d,j}$'s is ten. We have

$$Z(G_{CDBC}[2 \times m], v^2, v) = v^{2m+2} \left[\sum_{j=1}^5 (\bar{\lambda}_{2,1,j})^m + \bar{\kappa}^{(2)} \sum_{j=1}^4 (\bar{\lambda}_{2,2,j})^m + \bar{\kappa}^{(3)} \right] \quad (4.9)$$

where

$$\bar{\lambda}_{2,2,j} = \frac{1}{4} \left[7 + \eta\sqrt{5} + 4v \pm \left[2(19 + 7\eta\sqrt{5}) + 8(3 + \eta\sqrt{5})v \right]^{1/2} \right] \quad (4.10)$$

where $\eta = \pm 1$, yielding four possible terms. The $\bar{\lambda}_{2,1,j}$ are roots of a quintic equation which can be derived from the general quintic given in Ref. [21]. For $v = -2$, all of the roots (4.10) have unit modulus and this is also true of the roots of the above-mentioned quintic equation, so that all ten $\bar{\lambda}_{2,d,j}$ have $|\bar{\lambda}_{2,d,j}| = 1$. We show our results for \mathcal{B}_v and \mathcal{B}_Q in Figs. 2 and 3, together with partition function zeros calculated for a strip with length $L_x = 30$. (For this and other figures, some zeros have sufficiently large magnitudes so that they are not shown.) We find that the locus \mathcal{B}_v crosses the negative v plane at $v = -2$ and $v = -2 \cos(\pi/(2\ell + 1))$ for $\ell = 1, 2$, i.e., -1 , and $-2 \cos(\pi/5) = -(1 + \sqrt{5})/2 \simeq -1.618$. Correspondingly, \mathcal{B}_Q crosses the positive Q axis at the squares of these values, $4 \cos^2(\pi/(2\ell + 1))$ for $\ell = 0, 1, 2$, i.e., 4 , 1 , and $4 \cos^2(\pi/5) = (3 + \sqrt{5})/2 \simeq 2.618$. Two complex-conjugate curves on \mathcal{B} extend to complex infinity in the v and Q planes, rendering the loci noncompact in these variables. In contrast, \mathcal{B} is compact in the $1/v$ or $1/Q$ planes, and we show \mathcal{B} in the $1/Q$ plane in Fig. 4. The fact that \mathcal{B} extends to $1/Q = 0$ means that the free energy does not have a Taylor series expansion in $1/Q$. This feature is similar to the situation for the quantity $W = \lim_{n \rightarrow \infty} P(G, Q)^{1/n}$ for certain families of graphs [30]. The confluence of curves at $v = -2$ and thus $Q = 4$ reflects the degeneracy in magnitude of the ten $\bar{\lambda}_{2,d,j}$'s.

We comment on some additional features of \mathcal{B}_Q in Fig. 3. This locus contains a set of complex-conjugate arcs that extend from $Q = 4$ outward from the real axis, crossing the imaginary axis at $Q \simeq \pm 6.52i$ and ending at $Q \simeq -1.96 \pm 6.27i$. Along the real Q axis for $Q \geq 4$, the dominant term is $\bar{\lambda}_{2,1,max}$. A different $\bar{\lambda}_{2,1,max}$ is dominant in the region extending to complex infinity in the Q plane separated by curves on \mathcal{B}_Q from this wedge containing the interval $Q \geq 4$. In the region containing the real interval $Q_3 \leq Q \leq Q_5$, i.e., $1 \leq Q \leq (1/2)(3 + \sqrt{5}) \simeq 2.618$, $\bar{\lambda}_{2,2,max}$ is dominant, while in the region containing the real interval $Q_5 \leq Q \leq Q_1$, i.e., $(1/2)(3 + \sqrt{5}) \leq Q \leq 4$, $\bar{\lambda}_{2,3} = 1$ is dominant. The partition function also has several isolated zeros that are not on \mathcal{B}_Q . In addition to the zero at $Q = 0$, it has zeros in the interval $[0, 4]$ very near to $Q = Q_4 = 2$ and $Q = Q_6 = 3$. The zeros very near to Q_4 and Q_6 result from the fact that the coefficient $\bar{\kappa}^{(2)}$ that multiplies the dominant term $(\bar{\lambda}_{2,2,max})^m$ in the region around $Q = 2$ vanishes at $Q = 2$, and the coefficient $\bar{\kappa}^{(3)}$ that multiplies the dominant term $(\bar{\lambda}_{2,3})^m = 1$ in the region around $Q = 3$ vanishes at $Q = 3$. The partition function also has real zeros in the region $Q > 4$.

D. $L_y = 3$

For $L_y = 3$, from the exact calculation of $Z(G_{CDBC}[3 \times L_x], Q, v)$ performed for Ref. [21] we specialize to the manifold (1.4) and calculate the partition function zeros. Because of the large number of $\bar{\lambda}_{3,d,j}$'s (a total of 35) that enter, we do not list these explicitly here.

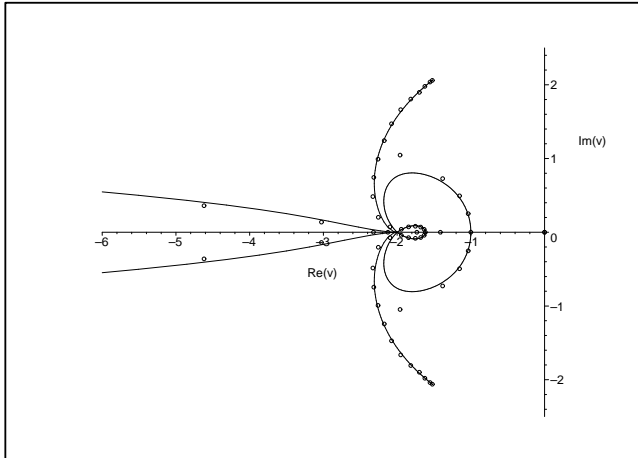


FIG. 2: Locus \mathcal{B}_v for the Potts model on a $2 \times \infty$ graph with CDBC and $Q = v^2$. Partition function zeros are shown for a graph of length $L_x = 30$.

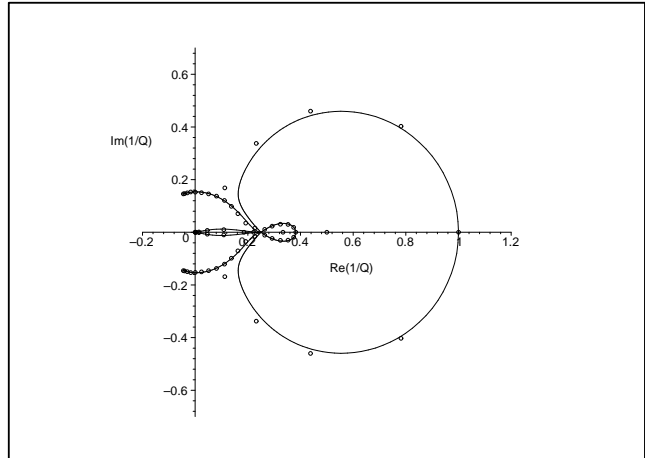


FIG. 4: Locus \mathcal{B} plotted in the $1/Q$ plane, for the Potts model on a $2 \times \infty$ graph with CDBC and $Q = v^2$. Partition function zeros are shown for a graph of length $L_x = 30$.

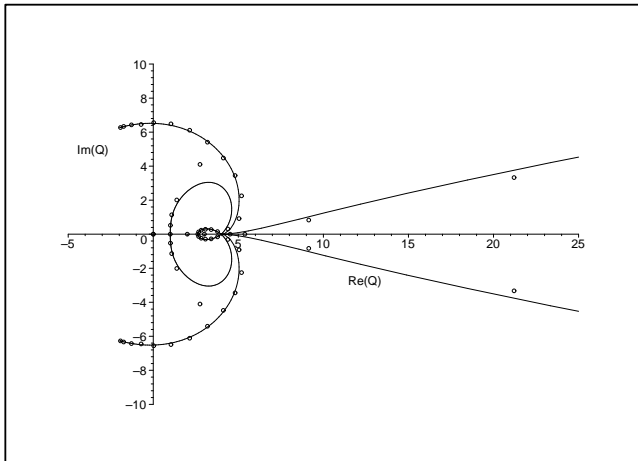


FIG. 3: Locus \mathcal{B}_Q for the Potts model on a $2 \times \infty$ graph with CDBC and $Q = v^2$. Partition function zeros are shown for a graph of length $L_x = 30$.

Having discussed above how the zeros in the v plane and the locus \mathcal{B}_v map to zeros and the locus \mathcal{B}_Q in the Q plane, we display our results only in the latter plane. In Fig. 5 we show a plot of zeros and \mathcal{B}_Q . To depict the portions of \mathcal{B}_Q that extend infinitely far from the origin, it is again useful to include, as Fig. 6, a plot of \mathcal{B} in the $1/Q$ plane, where it is compact. We find that in the interval $-2 \leq v \leq -1$ the locus \mathcal{B}_v crosses the negative real v

axis at $v = -2$ and $v = -2 \cos(\pi/(2\ell + 1))$ for $\ell = 1, 2, 3$, i.e., -1 , $-2 \cos(\pi/5) = -(1/2)(1 + \sqrt{5}) \simeq -1.618$, and $-2 \cos(\pi/7) \simeq -1.802$. Correspondingly, in the interval $1 \leq Q \leq 4$ the locus \mathcal{B}_Q crosses the positive Q axis at the squares of these values, $4 \cos^2(\pi/(2\ell + 1))$ for $\ell = 0, 1, 2, 3$, i.e., 4 , 1 , $4 \cos^2(\pi/5) = (3 + \sqrt{5})/2 \simeq 2.618$, and $4 \cos^2(\pi/7) \simeq 3.247$. For $L_x = 26$, there are zeros very close to $Q_4 = 2$, $Q_6 = 3$, and $Q_8 = 2 + \sqrt{2} \simeq 3.414$. Our exact results also show that the locus \mathcal{B}_v contains a semi-infinite line segment on the real axis extending leftward from $v = -2$ to $v = \infty$ and, correspondingly, \mathcal{B}_Q contains a semi-infinite line segment on the interval $4 \leq Q \leq \infty$. While the region boundary that includes $Q = 1$ and $Q = 4$ was convex in the neighborhood of $Q = 1$ for $L_y = 1$ and $L_y = 2$, it becomes concave in this neighborhood for $L_y = 3$ (and $L_y = 4$). This boundary also extends further outward from the real axis than for the lower values of L_y , reaching to roughly $\pm 4.23i$. The outermost finite complex-conjugate arcs reach farther away from the real axis than the analogous arcs for $L_y = 2$, crossing the imaginary axis at $Q \simeq \pm 10i$, and extend farther to the left, with arc endpoints at approximately $Q \simeq -6.8 \pm 4.8i$. The dominant terms are as follows: (i) two different $\bar{\lambda}_{3,1,max}$'s in the region containing the real interval $Q \geq 4$ and the separate region extending to complex infinity, (ii) $\bar{\lambda}_{3,2,max}$ in the region containing the interval $Q_3 \leq Q \leq Q_5$, (iii) $\bar{\lambda}_{3,3,max}$ in the region containing the interval $Q_5 \leq Q \leq Q_7$, i.e., approximately $2.618 < Q < 3.247$, and (iv) $\bar{\lambda}_{3,4} = 1$ in the region containing the interval $Q_7 \leq Q \leq Q_1 = 4$.

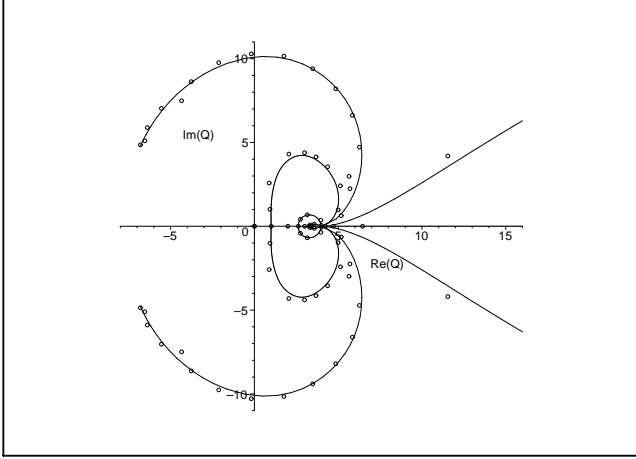


FIG. 5: Locus \mathcal{B}_Q for the Potts model on a $3 \times \infty$ graph with CDBC and $Q = v^2$. This locus includes a semi-infinite line segment in the interval $4 \leq Q \leq \infty$. Partition function zeros are shown for a graph of length $L_x = 26$.

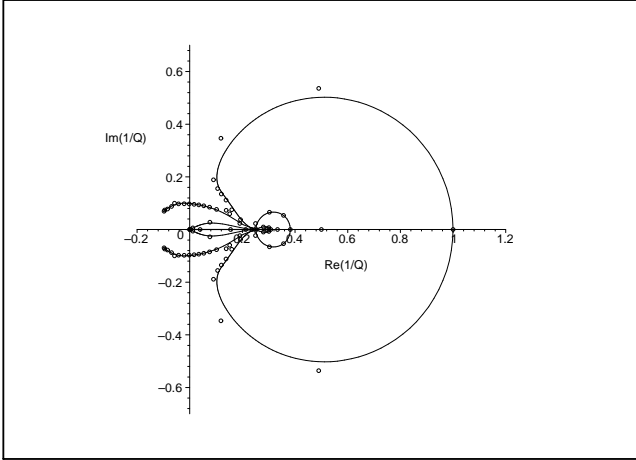


FIG. 6: Locus \mathcal{B} plotted in the $1/Q$ plane, for the Potts model on a $3 \times \infty$ graph with CDBC and $Q = v^2$. This locus includes a line segment in the interval $0 \leq 1/Q \leq 1/4$. Partition function zeros are shown for a graph of length $L_x = 26$.

E. $L_y = 4$

For the present work we have also calculated $Z(G_{CDBC}[4 \times L_x], Q, v)$ exactly for $Q = v^2$. Owing to the large number of $\lambda_{4,d,j}$'s (126 in total), we again do not list them here. We find that the resultant locus \mathcal{B}_v crosses the

negative real v axis at $v = -2$ and $v = -2 \cos(\pi/(2\ell+1))$ for $\ell = 1, 2, 3, 4$ and thus \mathcal{B}_Q crosses the positive Q axis at the squares of these values. The outer complex-conjugate arcs on \mathcal{B}_Q continue the trend observed for $L_y = 2, 3$ of having parts that extend farther from the real axis, crossing the imaginary axis at $Q \simeq \pm 13i$, but at the same time, having endpoints that move leftward and inward toward the real axis, so that these endpoints occur near to this axis. The dominant terms are as follows: (i) different $\bar{\lambda}_{4,1,max}$'s in the region containing the interval $Q \geq 4$ and the region extending to complex infinity, (ii) $\bar{\lambda}_{4,2,max}$ in the region containing the interval $Q_3 \leq Q \leq Q_5$, (iii) $\bar{\lambda}_{4,3,max}$ in the region containing the interval $Q_5 \leq Q \leq Q_7$, (iv) $\bar{\lambda}_{4,4,max}$ in the region containing the interval $Q_7 \leq Q \leq Q_9$, and (v) $\bar{\lambda}_{4,5} = 1$ in the region containing the interval $Q_9 \leq Q \leq Q_{10} = 4$. In addition to the isolated zero at $Q = Q_2 = 0$, the partition function also exhibits other isolated zeros not on \mathcal{B}_Q very close to $Q_4 = 2$, $Q_6 = 3$, $Q_8 = 2 + \sqrt{2} \simeq 3.414$, and $Q_{10} = (1/2)(5 + \sqrt{5}) \simeq 3.618$. The reason is again due to vanishing coefficients of dominant terms at these values of Q , as discussed above.

V. GENERAL PROPERTIES AND CONJECTURE FOR \mathcal{B} FOR ARBITRARY L_y

In our exact calculations on CDBC strips with widths $1 \leq L_y \leq 4$, we have discerned several systematic features which we generalize here. For the Potts model on self-dual cyclic strips of the square lattice of arbitrary width L_y , with Q and v satisfying eq. (1.4), in the limit $L_x \rightarrow \infty$, we conjecture that

- In the interval $-2 \leq v \leq -1$ the locus \mathcal{B}_v crosses the negative real v axis at $v = -2$ and

$$v = v_{2\ell+1} = -2 \cos\left(\frac{\pi}{2\ell+1}\right) \quad \text{for } 1 \leq \ell \leq L_y \quad (5.1)$$

For odd L_y this locus \mathcal{B}_v also includes the semi-infinite line segment

$$-\infty \leq v \leq -2. \quad (5.2)$$

- Hence, in the interval $1 \leq Q \leq 4$ the locus \mathcal{B}_Q crosses the Q axis at

$$Q = Q_{2\ell+1} = 4 \cos^2\left(\frac{\pi}{2\ell+1}\right) \quad \text{for } 0 \leq \ell \leq L_y \quad (5.3)$$

corresponding to the roots of unity given in eq. (2.11) with $r = 2\ell + 1$. For odd L_y the locus \mathcal{B}_Q also includes the semi-infinite line segment

$$4 \leq Q \leq \infty. \quad (5.4)$$

These properties do not preclude the possibility that, for sufficiently wide strips, the locus \mathcal{B}_Q may also cross the real Q axis at points in the intervals $Q < 0$ or $Q > 4$.

- For a strip of width L_y , the locus \mathcal{B}_v divides the v plane into at least $2L_y$ regions, and the locus \mathcal{B}_Q divides the Q plane into at least $2L_y$ regions. (Note that the number of regions into which \mathcal{B}_v and \mathcal{B}_Q divide their respective planes need not be equal; for a gedanken example, if \mathcal{B}_v were to contain just two complex-conjugate arcs emanating from $v = -2$ and crossing the imaginary v axis at $\pm ib_0$ with $b_0 \neq 0$ and then terminating in endpoints, this locus would not enclose a region in the v plane, but its image in the Q plane would enclose a region.)
- In the respective regions of the v and Q planes away from the real axis and extending to complex infinity, the dominant eigenvalue is $\bar{\lambda}_{L_y,1,max}$. In the region of the v plane containing the interval $-\infty \leq v \leq -2$, and equivalently, in the region of the Q plane containing the interval $4 \leq Q \leq \infty$, the dominant eigenvalue is a different $\bar{\lambda}_{L_y,1,max}$. The fact that this is different is evident from the equimodular curve separating this region in the v plane from the region extending to complex infinity, and similarly in the Q plane. For odd L_y , two eigenvalues from this set becomes degenerate on the real axis in the respective intervals $-\infty \leq v \leq -2$ and $4 \leq Q \leq \infty$, giving rise to the line segments on \mathcal{B}_v and \mathcal{B}_Q .
- Concerning the other regions that contain intervals of the real v and Q axes, the $L_y = 1$ case has been solved exactly above: in the region $-2 \leq v \leq -1$ and the corresponding region $1 \leq Q \leq 4$, $\bar{\lambda}_{1,2} = 1$ is dominant. For $L_y \geq 2$, in the region of the v plane containing the interval $v_{2k+3} \leq v \leq v_{2k+1}$, or equivalently in the region in the Q plane containing the interval $Q_{2k+1} \leq Q \leq Q_{2k+3}$ for $1 \leq k \leq L_y - 1$, $\bar{\lambda}_{L_y,k+1,max}$ is dominant. In the respective regions of the v and Q planes containing the intervals $-2 \leq v \leq v_{2L_y+1}$ and $Q_{2L_y+1} \leq Q \leq Q_1 = 4$, the dominant eigenvalue is $\bar{\lambda}_{L_y,L_y+1} = 1$.
- All of the $\bar{\lambda}_{L_y,d,j}$'s have the magnitude $|\bar{\lambda}_{L_y,d,j}| = 1$ at $v = -2$ or, in terms of Q , at $Q = 4$. Hence, all of the curves on \mathcal{B}_v meet at the point $v = -2$, and correspondingly, all of the curves on \mathcal{B}_Q meet at the point $Q = 4$.
- We next remark on zeros of $Z(G_{CDBC}[L_y \times L_x], v^2, v)$ that, in the limit $L_x \rightarrow \infty$, do not lie on \mathcal{B} , but instead are isolated (discrete). We have shown (so this is not just a conjecture) that there is an isolated zero at $v = 0$ of multiplicity at least $n + 1$ and hence also at $Q = 0$ with multiplicity that scales like $n/2$ for large n . In addition, from our exact results, we conjecture that for arbitrary

L_y , $Z(G_{CDBC}[L_y \times L_x], Q, v)$ with $Q = v^2$ has zeros close to the values

$$Q = Q_{2\ell} \quad \text{for } 1 \leq \ell \leq L_y + 1. \quad (5.5)$$

The basis of this inference and the way to understand this result is that these points are located within the region where the dominant eigenvalue of the transfer matrix, $\bar{\lambda}_{L_y,d,max}$, has a coefficient $\bar{\kappa}^{(d)}$ in eq. (3.2) that vanishes at the points (5.5), as is evident from eqs. (3.7) and (3.8).

For each of our plots showing the exact loci \mathcal{B}_Q on infinite-length strips of the square lattice with cyclic self-dual boundary conditions and $Q = v^2$, we have also shown zeros calculated for long finite strips for comparison. As was evident, these zeros lie close to the asymptotic loci \mathcal{B} . This comparison is especially easy to make for the plots of \mathcal{B} in the $1/Q$ plane, where it is compact; clearly, in the Q plane, the zeros for long finite sections cannot have arbitrarily large modulus and hence cannot track the portions of \mathcal{B} that extend infinitely far from the origin. It is also of interest to compare our results with calculations of zeros of $Z(G_{CDBC}[L \times L], Q, v)$ for finite $L \times L$ sections of the square lattice with $Q = v^2$ in Ref. [19]. Of course, for such a finite section, no locus \mathcal{B}_Q is defined; one is only able to make a rough comparison of patterns of zeros. One sees that a number of zeros in the Q plane occur at or near to certain Q_r 's [19] and that the zeros in the v and Q planes exhibit patterns suggesting the importance of the points $v = -2$ and $Q = 4$.

For general Q and v , the locus \mathcal{B}_ζ is compact for the infinite-length, finite-width self-dual strips of the square lattice [21]. We noted above how these strips share this property, along with their self-duality, with the (infinite) square lattice. In contrast, with these strips, when one restricts Q and v to satisfy the relation (1.4), \mathcal{B}_v and \mathcal{B}_Q become noncompact in the respective v and Q planes, passing through $1/v = 0$ and $1/Q = 0$.

VI. SELF-DUAL STRIPS WITH FREE LONGITUDINAL BOUNDARY CONDITIONS

We have also calculated $Z(G, v^2, v)$ on self-dual strips of the square lattice with free longitudinal boundary conditions. A strip of this type of length L_x and width L_y is constructed by adding an external vertex which is connected to each of the vertices on one horizontal side, say the upper one, and to each of the vertices on one vertical side, say the right-hand one, of the strip [16, 17, 21]. (Hence, the upper right-most vertex of the strip is connected to the external vertex with a double edge.) We denote this type of boundary condition as “free (self)-dual boundary condition”, abbreviated as FDBC, and the graph as $G_{FDBC}[L_y \times L_x]$.

For the strip $G_{FDBC}[1 \times m]$ we use our previous exact calculation of Z [20, 21] and restrict Q and v to satisfy (1.4). The partition function depends only on (the m 'th

powers of) the $\bar{\lambda}_{1,1,j}$ in eq. (4.2). As is evident from eq. (4.2), these are equal in magnitude for real $v \leq -5/4$, and consequently, \mathcal{B}_v is the semi-infinite line segment extending from $v = -5/4$ to $v = -\infty$. The image of this in the Q plane, \mathcal{B}_Q , is the semi-infinite line segment from $Q = (5/4)^2 = 1.5625$ to $Q = \infty$. Thus, as was the case with the infinite-length CDBC strips, the loci \mathcal{B}_v and \mathcal{B}_Q are noncompact in the respective v and Q planes. For FDDB strips with larger widths we find that \mathcal{B}_v and \mathcal{B}_Q consist of arcs and line segments and generically exhibit the above noncompactness.

VII. OTHER STRIPS

We have considered strips of the square lattice with free (F) and periodic (P) boundary conditions in the transverse and longitudinal directions, which we label in an obvious manner, e.g., $(FBC_y, FBC_x) = \text{free}$, $(FBC_y, PBC_x) = \text{cyclic}$, $(PBC_y, FBC_x) = \text{cylindrical}$, and $(PBC_y, PBC_x) = \text{toroidal}$. We observe that for the cyclic square-lattice strips that we have studied, \mathcal{B}_Q crosses the real axis at a set of points including $Q_1 = 4$ and $Q_{2\ell}$ for $1 \leq \ell \leq L_y$. We find that for some strips \mathcal{B}_Q also crosses the real axis for $Q < 0$ or $Q > 4$.

In addition, we have calculated the loci \mathcal{B} for infinite-length strips of the triangular lattice, with Q and v restricted to satisfy the relation $Q = v^2(v + 3)$, which is the phase transition condition for the Potts ferromagnetic on the triangular lattice. As in the case of the cyclic and toroidal square-lattice strips, we find that for the case of periodic boundary longitudinal conditions, \mathcal{B}_Q crosses the real axis at $Q = 0$ and $Q = 4$ as well as at other points that depend on the type of strip. The intersections of \mathcal{B}_Q with the real axis sometimes include finite line segments. A detailed discussion of our results for these other lattice strips will be presented elsewhere.

VIII. RELATION TO \mathcal{B} FOR GENERAL Q, v

It is interesting to observe the connections between the loci that we have determined for the $Q = v^2$ case to the continuous accumulation loci \mathcal{B} in other variables, such as (i) complex v for fixed Q ; (ii) complex Q for fixed v ; and (iii) complex ζ for, e.g., various values of Q . We concentrate on the CDBC strips and comment briefly on others. In Ref. [21] we displayed the loci in the ζ plane for several values of Q in Ref. [21]. In relating these results to our present ones, one must take account of the noncommutativity (3.11). Let us consider, for example, the CDBC strip of width $L_y = 1$. Figs. 9, 11, 12, and 13 of that paper gave \mathcal{B}_ζ for $Q = 2, 4, 5$, and 100, calculated by first setting Q equal to the given value, and then taking $L_x \rightarrow \infty$; these plots show that this locus passes through $\zeta = -1$, and hence our special case $Q = v^2$. This agrees with our present finding that for this special case, \mathcal{B}_Q passes through $Q = Q_1 = 4$, and contains a

semi-infinite line segment on the interval $4 \leq Q \leq \infty$. In the case $Q = 2$, the fact that the locus was calculated in Ref. [21] by first setting Q equal to this value and then taking $L_x \rightarrow \infty$ explains why the locus \mathcal{B}_ζ in Ref. [20] passes through $\zeta = -1$, while our locus \mathcal{B}_Q , calculated by first taking $L_x \rightarrow \infty$, does not pass through $Q = 2$; the reason is that these limits do not commute. The origin of this noncommutativity is clear: setting $Q = 2$ first means that $\bar{\kappa}^{(2)} = 0$, and this annihilates what would be the dominant term in the vicinity of $v = -\sqrt{2}$, $Q = 2$, namely, $(\bar{\lambda}_{1,2})^{L_x} = 1$. For $Q = 3$, the locus \mathcal{B}_ζ , shown in Fig. 10 of Ref. [21] does not pass through $\zeta = -1$, which again agrees with our finding that the point $Q = 3$ is not on \mathcal{B}_Q for the special case $Q = v^2$. Similar comparisons can be made for the results shown in Ref. [21] for CDBC strips with widths $L_y = 2$ and $L_y = 3$.

The case of self-dual strips of the square lattice with free longitudinal boundary conditions was also studied in Ref. [21]. For example, as is shown in Figs. 2-6 of Ref. [21], as Q increases from 1 to $(5/4)^2$, two complex-conjugate arcs on \mathcal{B}_ζ elongate and two of their endpoints come together and pinch the real axis at $\zeta = -1$; for $Q \geq (5/4)^2$, the locus \mathcal{B}_ζ continues to pass through $\zeta = -1$. Again, this agrees with our present analysis, where we have found that for $Q = v^2$, \mathcal{B}_v and \mathcal{B}_Q contain the respective semi-infinite line segments $-\infty \leq v \leq -5/4$ and $(5/4)^2 \leq Q \leq \infty$. Similar connections can be made for other strips.

We can also relate our present results to the loci \mathcal{B}_Q that we previously determined in the Q plane for the $L_x \rightarrow \infty$ limits of chromatic polynomials $P(G, Q) = Z(G, Q, -1)$ of various lattice strip graphs with CDBC and FDDB [20]. For CDBC strips we found that \mathcal{B} crossed the real Q axis at $Q = Q_3 = 1$, which lies on the submanifold $Q = v^2$ and agrees with our present result that for Q and v restricted to this submanifold, \mathcal{B}_v passes through $v = -1$ (see Figs. 2-4 of Ref. [20]). For strips of the square lattice with cyclic and toroidal (and Möbius and Klein-bottle) boundary conditions, we found that for $v = -1$, \mathcal{B}_Q does not pass through $Q = 1$. This agrees with our finding that for these strips, with $Q = v^2$, \mathcal{B}_v and \mathcal{B}_Q do not pass through the respective points $v = -1$ and $Q = 1$.

IX. CONCLUSIONS

In conclusion, we have presented exact results for the continuous accumulation set \mathcal{B} of the locus of zeros of the Potts model partition function for the infinite-length limits of self-dual cyclic square-lattice strips of various widths L_y with Q and v satisfying the relation $Q = v^2$. For these quasi-one-dimensional strips, one motivation for interest in this submanifold of values of Q and v is its invariance under a duality transformation. From our exact calculations we have discerned several general features and have incorporated them in a conjecture applicable for arbitrary width L_y . We have also presented

some results on \mathcal{B} for self-dual strips of the square lattice with free longitudinal boundary conditions. Further studies of these loci for other strips are worthwhile. The findings add to the set of exact results that one has for the Potts model on the $n \rightarrow \infty$ limits of lattice graphs.

NSC-94-2112-M-006-013 (S.-C.C.).

X. ACKNOWLEDGMENTS

This research was partially supported by the NSF grant PHY-00-98527 (R.S.) and the Taiwan NSC grant

-
- [1] F. Y. Wu, Rev. Mod. Phys. **54**, 235 (1982).
 [2] R. J. Baxter, *Exactly Solved Models in Statistical Mechanics* (Academic Press, New York, 1982).
 [3] P. Martin, *Potts Models and Related Problems in Statistical Mechanics* (World Scientific: Singapore, 1991).
 [4] References to some of our earlier works and other related papers in this area can be found in S.-C. Chang and R. Shrock, Physica A **346**, 400 (2005); *ibid.* **347**, 314 (2005). We switch notation here relative to our previous papers, using Q for what was denoted q there in order to follow conventional notation for q as a root of unity.
 [5] P. Kasteleyn and C. Fortuin, J. Phys. Soc. Jpn. **26** (Suppl.) 11 (1969); C. Fortuin and P. Kasteleyn, Physica **57**, 536 (1972).
 [6] H. W. J. Blöte and M. P. Nightingale, Physica A **112**, 405 (1982).
 [7] The coefficients are, of course, not just real, but are non-negative integers; however, the latter property is not needed for the invariance noted here.
 [8] W. T. Tutte, J. Combin. Theory **9**, 289 (1970).
 [9] W. T. Tutte, “Chromials”, in Lecture Notes in Mathematics, v. 411, p. 243 (1974); W. T. Tutte, *Graph Theory*, vol. 21 of Encyclopedia of Mathematics and Applications (Addison-Wesley, Menlo Park, 1984).
 [10] H. N. V. Temperley and E. H. Lieb, Proc. R. Soc. A **322**, 251 (1971).
 [11] S. Beraha, J. Kahane, and N. Weiss, J. Combin. Theory B **27**, 1 (1979); J. Combin. Theory B **28**, 52 (1980).
 [12] H. Saleur, Commun. Math. Phys. **132**, 657 (1990); Nucl. Phys. B **360**, 219 (1991).
 [13] P. Martin, J. Phys. A **20**, L399 (1987).
 [14] Indeed, more generally, representations of quantum algebras have special properties when the deformation parameter, analogous to q here, is a root of unity. Reviews include G. Lusztig, *Introduction to Quantum Groups*, Prog. Math. **110** (Birkhäuser, Boston, 1993); C. Kassel, *Quantum Groups* (Springer, New York, 1995); and V. Chari and A. Pressley, *Guide to Quantum Groups* (Cambridge Univ. Press, Cambridge, 1994).
 [15] Note that for $L_x = 2$, the graph has two-fold multiple horizontal edges joining adjacent vertices.
 [16] C. N. Chen, C. K. Hu, and F. Y. Wu, Phys. Rev. Lett. **76**, 169 (1996).
 [17] V. Matveev and R. Shrock, Phys. Rev. E **54**, 6174 (1996). In this paper, the CDBC and FDBC strips were denoted DBC2 and DBC1.
 [18] W. T. Lu and F. Y. Wu, Physica A **258**, 157 (1998).
 [19] S.-Y. Kim and R. Creswick, Phys. Rev. E **63**, 066107 (2001).
 [20] S.-C. Chang and R. Shrock, Physica A **301**, 301 (2001).
 [21] S.-C. Chang and R. Shrock, Phys. Rev. E **64**, 066116 (2001).
 [22] S.-C. Chang and R. Shrock, Physica A **301**, 196 (2001).
 [23] S.-C. Chang and R. Shrock, Physica A **296**, 131 (2001).
 [24] R. Shrock, Physica A **283**, 388 (2000).
 [25] S.-C. Chang and R. Shrock, Physica A **296**, 234 (2001).
 [26] S.-C. Chang and R. Shrock, Physica A **286**, 189 (2000).
 [27] S.-C. Chang and R. Shrock, Physica A **296**, 183 (2001).
 [28] S.-C. Chang and R. Shrock, Int. J. Mod. Phys. B **15**, 443 (2001).
 [29] S.-C. Chang, J. Salas, and R. Shrock, J. Stat. Phys. **107** 1207 (2002).
 [30] R. C. Read and G. F. Royle, in *Graph Theory, Combinatorics, and Applications* (Wiley, New York, 1991), v. 2, p. 1009; R. Shrock and S.-H. Tsai, Phys. Rev. E **56**, 3935 (1997); J. Phys. A **31**, 9641 (1998); A. Sokal, Combin. Prob. Comput. **10**, 41 (2001).